

**Calculations executed for the 3-bladed rotor of the VIRYA-1.02 windmill ( $\lambda_d = 3.5$ ,  
15° folded stainless steel blades) meant to be coupled to the VIRYA-1 generator**

ing. A. Kragten

June 2019  
reviewed December 2019

KD 678

It is allowed to copy this report for private use. It is allowed to use the rotor given in this report for the VIRYA-1.02 windmill but this windmill has not been tested by Kragten Design. No responsibility is accepted for use of the VIRYA-1.02 windmill or any of its parts.

Engineering office Kragten Design  
Populierenlaan 51  
5492 SG Sint-Oedenrode  
The Netherlands  
telephone: +31 413 475770  
e-mail: [info@kdwindturbines.nl](mailto:info@kdwindturbines.nl)  
website: [www.kdwindturbines.nl](http://www.kdwindturbines.nl)

| Contains |   | page |
|----------|---|------|
| 1        | Introduction  | 3    |
| 2        | Description of the rotor of the VIRYA-1.02 windmill                               | 3    |
| 3        | Calculations of the rotor geometry  | 4    |
| 4        | Determination of the $C_p$ - $\lambda$ and the $C_q$ - $\lambda$ curves           | 5    |
| 5        | Determination of the P-n curves, the optimum cubic line and the $P_{el}$ -V curve | 7    |
| 6        | Generator measurements  | 10   |
|          | 6.1 General   | 10   |
|          | 6.2 Measuring results   | 12   |
| 7        | Discussion of the measuring results   | 15   |
| 8        | Ideas about an alternative stator for the VIRYA-1.02                              | 17   |
| 9        | References  | 18   |
|          | Appendix 1  |      |
|          | Drawing VIRYA-1.02 rotor  |      |

## 1 Introduction

The 3-bladed VIRYA-1.02 is an alternative for the 2-bladed VIRYA-1. The rotor blades of the VIRYA-1 have a 7.14 % cambered airfoil. Cambering requires a special press. For twisting of the blades, special tools for cambered blades are needed. These tools are relatively expensive if only one windmill is built. In this report KD 678 it is investigated if it is possible to use rectangular blades with folded sides because now much simpler and cheaper tools are needed.

The VIRYA-1.02 makes use of the same 8-pole axial flux generator which is also used for the third version of the VIRYA-1 and which is described in report KD 679 (ref. 1). KD 679 includes drawings of the armature sheet, the stator sheet and the coils. This generator uses the front wheel hub of a mountain bike as generator housing.

The VIRYA-1.02 and the VIRYA-1 make use of the head, the tower pipe and the safety system of the 3-bladed VIRYA-1.04. The rotor calculations of the VIRYA-1.04 are given in report KD 518 (ref. 2). The drawings of the VIRYA-1.04 are given in a separate manual (ref. 3). This manual includes the drawings of the head. The VIRYA-1.04 makes use of a Nexus hub dynamo but the maximum power of this dynamo is only about 6 W for 12 V battery charging. The rotor diameter of the VIRYA-1.02 is chosen a little smaller than that of the VIRYA-1.04 to make an efficient use of the chosen materials. The rated wind speed is about 8 m/s for a 1.5 mm aluminium vane blade.

## 2 Description of the rotor of the VIRYA-1.02 windmill

The 3-bladed rotor of the VIRYA-1.02 windmill has a diameter  $D = 1.02$  m and a design tip speed ratio  $\lambda_d = 3.5$ . Advantages of a 3-bladed rotor are that the gyroscopic moment in the rotor shaft is not fluctuating and that a 3-bladed rotor looks nicer than a 2-bladed rotor.

The rotor has three blades which are made of rectangular stainless steel sheets with size  $125 * 416 * 1$  mm. 60 blades can be made out of a standard sheet of  $1.25 * 2.5$  m with almost no waste material. All four corners of a blade are rounded with  $r = 5$  mm. The blade has no camber but in stead of camber, both 27.5 mm wide sides are bent forwards over an angle of  $15^\circ$ . It is expected that the aerodynamic characteristics of this special airfoil are about the same as for a 7.14 % cambered airfoil. The chord  $c$  is a little smaller than the strip width because of the bent sides. Assume  $c = 123$  mm = 0.123 m. A blade is twisted linear.

The blades are connected to the generator by a stainless steel hub plate made out of 1.5 mm sheet. The hub plate has three 120 mm long and 70 mm wide ears. The overlap in between an ear and a blade is 26 mm resulting in a rotor diameter of 1020 mm. A blade is connected to the hub plate by two stainless steel bolts M5 \* 10, two self locking nuts M5 and two washers. The inner 30 mm of the hub plate is flat. The ear is twisted in between this flat side and the blade root to get the correct blade setting angle. The rotor mass is about 1.5 kg.

The aluminium front wheel hub of a mountain bike has two identical flanges. For connection of the spokes, each flange has 18, 2.6 mm holes at a pitch angle of  $20^\circ$  and at a pitch circle diameter of 45 mm. The hub plate is connected to the front flange and six 2.6 mm holes in this flange are enlarged up to 4 mm. The front flange has a collar with a diameter of 35 mm. A 35.2 mm central hole is made in the hub plate for centring on the collar. The hub plate is connected to the front flange by six stainless steel bolts M4 \* 10, six self locking nuts M4 and six washers. The armature sheet of the generator is connected to the back flange and six 2.6 mm holes in this flange are enlarged up to 4 mm.

It is expected that it is not necessary to balance the rotor if the hole patterns in the blades and the hub plate are made accurately. However, if there is some imbalance, this can be corrected by grinding a little from the heaviest blade tip. The drawing of the rotor with drawing number 1902-01 is given in appendix 1.

### 3 Calculation of the rotor geometry

The rotor geometry is determined using the method and the formulas as given in report KD 35 (ref. 4). This report (KD 678) has its own formula numbering. Substitution of  $\lambda_d = 3.5$  and  $R = 0.51$  m in formula (5.1) of KD 35 gives:

$$\lambda_{rd} = 6.8627 * r \quad (-) \quad (1)$$

Formula's (5.2) and (5.3) of KD 35 stay the same so:

$$\beta = \phi - \alpha \quad (^\circ) \quad (2)$$

$$\phi = 2/3 \arctan 1 / \lambda_{rd} \quad (^\circ) \quad (3)$$

Substitution of  $B = 3$  and  $c = 0.123$  m in formula (5.4) of KD 35 gives:

$$C_l = 68.110 r (1 - \cos\phi) \quad (-) \quad (4)$$

Substitution of  $V = 5$  m/s and  $c = 0.123$  m in formula (5.5) of KD 35 gives:

$$Re_r = 0.410 * 10^5 * \sqrt{(\lambda_{rd}^2 + 4/9)} \quad (-) \quad (5)$$

The blade is calculated for six stations A till F which have a distance of 0.078 m. Station A corresponds to the blade tip. Station F corresponds to the end of a hub plate ear. The blade has a constant chord and the calculations therefore correspond with the example as given in chapter 5.4.2 of KD 35. This means that the blade is designed with a low lift coefficient at the tip and with a high lift coefficient at the root. First the theoretical values are determined for  $C_l$ ,  $\alpha$  and  $\beta$  and next  $\beta$  is linearised such that the twist is constant and that the linearised values for the outer part of the blade correspond as good as possible with the theoretical values. The result of the calculations is given in table 1.

Although the blade has  $15^\circ$  bent sides, it is assumed that the aerodynamic characteristics for 7.14 % camber can be used. Aerodynamic characteristics for 7.14 % camber are given in report KD 398 (ref. 5). The Reynolds values for the stations are calculated for a wind speed of 5 m/s because this is a reasonable wind speed for a windmill which is designed for a rated wind speed of 8 m/s.

| station | r (m) | $\lambda_{rd}$ (-) | $\phi$ (°) | c (m) | $C_{lth}$ (-) | $C_{lin}$ (-) | $Re_r * 10^{-5}$<br>V = 5 m/s | $Re * 10^{-5}$<br>7.14 % | $\alpha_{th}$ (°) | $\alpha_{lin}$ (°) | $\beta_{th}$ (°) | $\beta_{lin}$ (°) | $C_d/C_{lin}$ (-) |
|---------|-------|--------------------|------------|-------|---------------|---------------|-------------------------------|--------------------------|-------------------|--------------------|------------------|-------------------|-------------------|
| A       | 0.51  | 3.5                | 10.6       | 0.123 | 0.60          | 0.70          | 1.46                          | 1.7                      | 0.0               | 0.6                | 10.6             | 10                | 0.051             |
| B       | 0.432 | 2.965              | 12.4       | 0.123 | 0.69          | 0.65          | 1.25                          | 1.2                      | 0.9               | 0.6                | 11.5             | 11.8              | 0.043             |
| C       | 0.354 | 2.429              | 14.9       | 0.123 | 0.81          | 0.78          | 1.03                          | 1.2                      | 1.7               | 1.3                | 13.2             | 13.6              | 0.039             |
| D       | 0.276 | 1.894              | 18.6       | 0.123 | 0.98          | 1.01          | 0.86                          | 1.2                      | 3.0               | 3.2                | 15.6             | 15.4              | 0.030             |
| E       | 0.198 | 1.359              | 24.2       | 0.123 | 1.19          | 1.31          | 0.62                          | 1.2                      | 5.1               | 7.0                | 19.1             | 17.2              | 0.051             |
| F       | 0.12  | 0.824              | 33.7       | 0.123 | 1.37          | 1.30          | 0.43                          | 1.2                      | 8.2               | 14.7               | 25.5             | 19                | 0.23              |

table 1 Calculation of the blade geometry of the VIRYA-1.02 rotor

The theoretical blade angle  $\beta_{th}$  varies in between  $10.6^\circ$  and  $25.5^\circ$ . If the blade angle is taken  $10^\circ$  at the blade tip and  $19^\circ$  at the blade root, the linearised blade angles are lying close to the theoretical values for the most important outer part of the blade. A hub plate ear is twisted  $19^\circ$  right hand in between the flat inner 30 mm and station F to get the correct blade angle at station F (the rotor is rotating right hand). A blade is twisted  $9^\circ$  left hand in between station A and station F to get a blade angle of  $10^\circ$  at the blade tip.

#### 4 Determination of the $C_p$ - $\lambda$ and the $C_q$ - $\lambda$ curves

The determination of the  $C_p$ - $\lambda$  and  $C_q$ - $\lambda$  curves is given in chapter 6 of KD 35. The average  $C_d/C_l$  ratio for the outer part of the blade is about 0.04. However, as the used airfoil is not a 7.14 % cambered sheet but a flat sheet with 15° bevelled edges, a higher value of 0.07 is chosen. Figure 4.7 of KD 35 (for  $B = 3$ ) and  $\lambda_{opt} = 3.5$  and  $C_d/C_l = 0.07$  gives  $C_{p\ th} = 0.38$ .

The blade is stalling at station F. So for the calculation of  $C_{p\ max}$ , not the real blade length  $k = 0.416$  m is taken but only a length up to 0.04 m outside station F. This gives an effective blade length  $k' = 0.35$  m. Substitution of  $C_{p\ th} = 0.38$ ,  $R = 0.51$  m and  $k = k' = 0.35$  m in formula 6.3 of KD 35 gives  $C_{p\ max} = 0.34$ .  $C_{q\ opt} = C_{p\ max} / \lambda_{opt} = 0.34 / 3.5 = 0.0971$ .

Substitution of  $\lambda_{opt} = \lambda_d = 3.5$  in formula 6.4 of KD 35 gives  $\lambda_{unl} = 5.6$ .

The starting torque coefficient is calculated with formula 6.12 of KD 35 which is copied as formula 6.

$$C_{q\ start} = 0.75 * B * (R - 1/2k) * C_l * c * k / \pi R^3 \quad (-) \quad (6)$$

The average blade angle  $\beta = 14.5^\circ$ . For a non rotating rotor, the angle  $\phi = 90^\circ$ . The average angle of attack  $\alpha$  is therefore  $90^\circ - 14.5^\circ = 75.5^\circ$ . The  $C_l$ - $\alpha$  curve for large angles  $\alpha$  is given in figure 5 of report KD 398 for 10 % camber. It is assumed that this curve can also be used for a stalling airfoil with 15° folded sides. For  $\alpha = 75.5^\circ$  it can be read that  $C_l = 0.49$ . The whole airfoil is stalling at stand still position, so now the real blade length  $k = 0.416$  m is taken.

Substitution of  $B = 3$ ,  $R = 0.51$  m,  $k = 0.416$  m,  $C_l = 0.49$  and  $c = 0.123$  m in formula 6 gives that  $C_{q\ start} = 0.041$ . The real starting torque coefficient will be somewhat lower because the average blade angle was used. Assume  $C_{q\ start} = 0.035$ . For the ratio in between the starting torque and the optimum torque we find that it is  $0.035 / 0.0971 = 0.36$ . This is rather high for a rotor with a design tip speed ratio of 3.5.

The starting wind speed  $V_{start}$  of the rotor is calculated with formula 8.6 of KD 35 which is given by:

$$V_{start} = \sqrt{\left( \frac{Q_s}{C_{q\ start} * 1/2\rho * \pi R^3} \right)} \quad (\text{m/s}) \quad (7)$$

The sticking torque  $Q_s$  of the generator is very low at  $n = 0$  rpm because it is only caused by the friction of the bearings. It is increasing slowly at increasing rotational speeds because of the eddy currents in the steel stator sheet. The unloaded  $Q$ - $n$  curve has been measured and is given in figure 7 of KD 626. It is about 0.02 Nm at stand still position. Substitution of  $Q_s = 0.02$  Nm,  $C_{q\ start} = 0.035$ ,  $\rho = 1.2$  kg/m<sup>3</sup> and  $R = 0.51$  m in formula 7 gives that  $V_{start} = 1.5$  m/s which is very low. The  $Q$ - $n$  curve of the rotor will rise faster at low rotational speeds than the unloaded  $Q$ - $n$  curve of the generator, so the rotor will really start at  $V = 1.5$  m/s. A starting wind speed of 1.5 m/s is lower than for the VIRYA-1 rotor for which  $V_{start}$  is about 2 m/s. The starting wind speed of the VIRYA-1.04 is about 2.6 m/s, so a lot higher. So the starting behaviour of the VIRYA-1.02 will be very good and the VIRYA-1.02 can therefore be used in regions with low wind speeds.

The VIRYA-1.02 has a design tip speed ratio of 3.5 in stead of 4.25 and a rated wind speed of 8 m/s in stead 9 m/s for the VIRYA-1, so the maximum tip speed of the VIRYA-1.02 will be lower. But an airfoil with 15° folded sides may have more turbulence than a 7.14 % cambered sheet and therefore it is expected that the noise production is about equal.

In chapter 6.4 of KD 35 it is explained how rather accurate  $C_p$ - $\lambda$  and  $C_q$ - $\lambda$  curves can be determined if only two points of the  $C_p$ - $\lambda$  curve and one point of the  $C_q$ - $\lambda$  curve are known. The first part of the  $C_q$ - $\lambda$  curve is determined according to KD 35 by drawing an S-shaped line which is horizontal for  $\lambda = 0$ .

Kragten Design developed a method with which the value of  $C_q$  for low values of  $\lambda$  can be determined (see report KD 97 ref. 6). With this method, it can be determined that the  $C_q$ - $\lambda$  curve is directly rising for low values of  $\lambda$  if a 7.14 % cambered sheet airfoil is used. It is assumed that this is also true for the chosen airfoils with  $15^\circ$  folded sides. This effect has been taken into account and the estimated  $C_p$ - $\lambda$  and  $C_q$ - $\lambda$  curves for the VIRYA-1.02 rotor are given in figure 1 and 2.

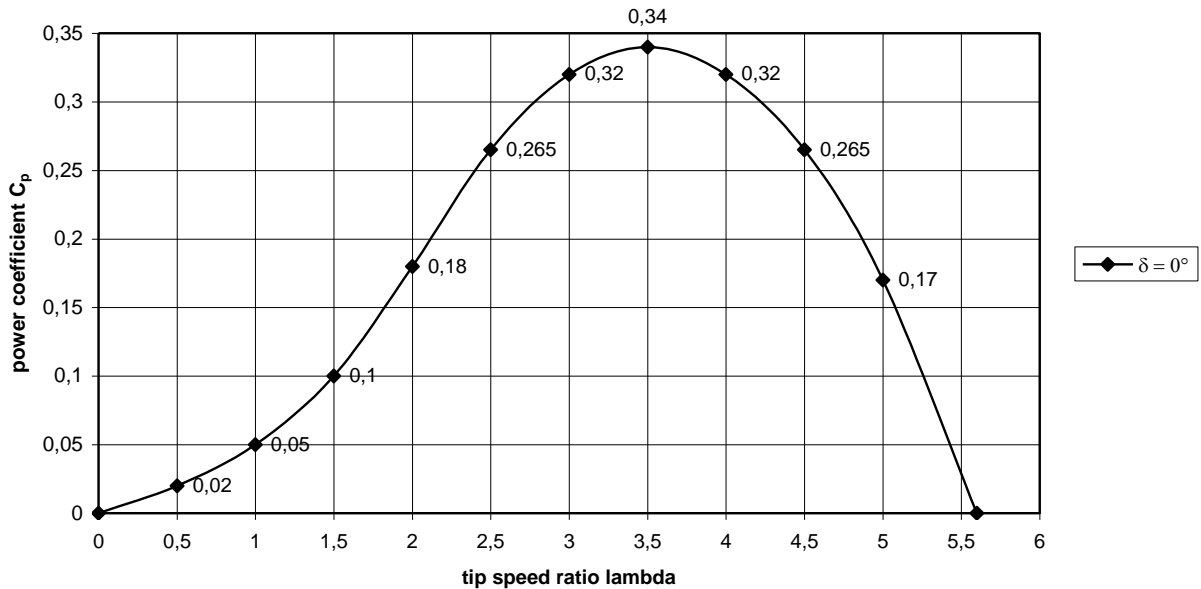


fig. 1 Estimated  $C_p$ - $\lambda$  curve for the VIRYA-1.02 rotor for the wind direction perpendicular to the rotor ( $\delta = 0^\circ$ )

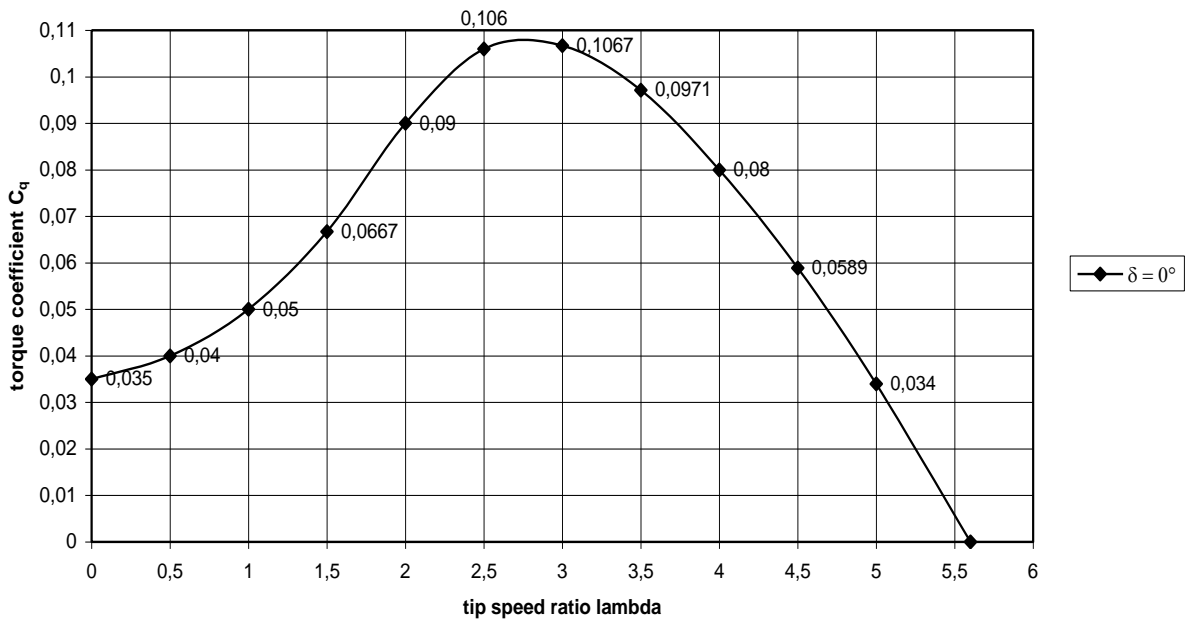


fig. 2 Estimated  $C_q$ - $\lambda$  curve for the VIRYA-1.02 rotor for the wind direction perpendicular to the rotor ( $\delta = 0^\circ$ )

## 5 Determination of the P-n curves, the optimum cubic line and the $P_{el}$ -V curve

The determination of the P-n curves of a windmill rotor is described in chapter 8 of KD 35. One needs a  $C_p$ - $\lambda$  curve of the rotor and the  $\delta$ -V curve of the safety system together with the formulas for the power P and the rotational speed n. The  $C_p$ - $\lambda$  curve is given in figure 1. The  $\delta$ -V curve for a 1.5 mm aluminium is estimated on the basis of the proven  $\delta$ -V curves of the VIRYA-1.8 and 2.2S windmills which have a 1 mm stainless steel vane blade and which have a rated wind speed of about 11 m/s. The estimated  $\delta$ -V curve for a 1.5 mm aluminium vane blade is given in figure 3.

The head starts to turn away at a wind speed of about 5 m/s. For wind speeds above 8 m/s it is supposed that the head turns out of the wind such that the component of the wind speed perpendicular to the rotor plane, is staying constant. The P-n curve for 8 m/s will therefore also be valid for wind speeds higher than 8 m/s.

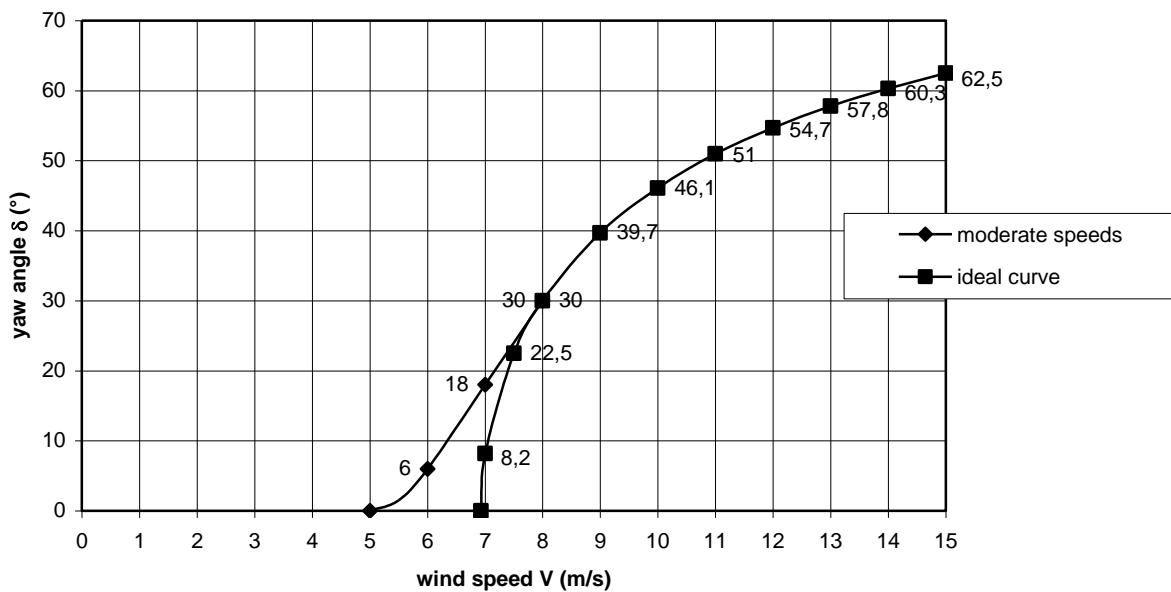


fig. 3 Estimated  $\delta$ -V curve VIRYA-1.02 for a 1.5 mm aluminium vane blade

The P-n curves are used to check the matching with the  $P_{mech}$ -n curve of the generator for a certain gear ratio  $i$  (the VIRYA-1.02 has no gearing so  $i = 1$ ). Because the P-n curve for low values of  $\lambda$  appears to lie very close to each other, the P-n curves are not determined for very low values of  $\lambda$ . The P-n curves are determined for  $C_p$  values belonging to  $\lambda$  is 2, 2.5, 3, 3.5, 4, 4.5, 5 and 5.6 (see figure 1). The P-n curves are determined for wind the speeds 2, 3, 4, 5, 6, 7 and 8 m/s. At high wind speeds the rotor is turned out of the wind by a yaw angle  $\delta$  and therefore the formulas for P and n are used which are given in chapter 7 of KD 35.

Substitution of  $R = 0.51$  m in formula 7.1 of KD 35 gives:

$$n = 18.724 * \lambda * \cos\delta * V \quad (\text{rpm}) \quad (8)$$

Substitution of  $\rho = 1.2$  kg / m<sup>3</sup> and  $R = 0.51$  m in formula 7.10 of KD 35 gives:

$$P = 0.4903 * C_p * \cos^3\delta * V^3 \quad (\text{W}) \quad (9)$$

For a certain wind speed, for instance  $V = 3$  m/s, related values of  $C_p$  and  $\lambda$  are substituted in formula 8 and 9 and this gives the P-n curve for that wind speed.

| $\lambda$ | $C_p$ | V = 2 m/s<br>$\delta = 0^\circ$ |       | V = 3 m/s<br>$\delta = 0^\circ$ |       | V = 4 m/s<br>$\delta = 0^\circ$ |       | V = 5 m/s<br>$\delta = 0^\circ$ |       | V = 6 m/s<br>$\delta = 6^\circ$ |           | V = 7 m/s<br>$\delta = 18^\circ$ |           | V = 8 m/s<br>$\delta = 30^\circ$ |           |
|-----------|-------|---------------------------------|-------|---------------------------------|-------|---------------------------------|-------|---------------------------------|-------|---------------------------------|-----------|----------------------------------|-----------|----------------------------------|-----------|
|           |       | n (rpm)                         | P (W) | $n_s$ (rpm)                     | $P_s$ (W) | $n_s$ (rpm)                      | $P_s$ (W) | $n_s$ (rpm)                      | $P_s$ (W) |
| 2         | 0.18  | 74.9                            | 0.71  | 112.3                           | 2.38  | 149.8                           | 5.65  | 187.2                           | 11.03 | 223.5                           | 18.75     | 249.3                            | 26.04     | 259.4                            | 29.35     |
| 2.5       | 0.265 | 93.6                            | 1.04  | 140.4                           | 3.51  | 187.2                           | 8.32  | 234.1                           | 16.24 | 279.3                           | 27.61     | 311.6                            | 38.34     | 324.3                            | 43.21     |
| 3         | 0.32  | 112.3                           | 1.26  | 168.5                           | 4.24  | 224.7                           | 10.04 | 280.9                           | 19.61 | 335.2                           | 33.34     | 374.0                            | 46.29     | 389.2                            | 52.18     |
| 3.5       | 0.34  | 131.1                           | 1.33  | 196.6                           | 4.50  | 262.1                           | 10.67 | 327.7                           | 20.84 | 391.0                           | 35.42     | 436.3                            | 49.19     | 454.0                            | 55.44     |
| 4         | 0.32  | 149.8                           | 1.26  | 224.7                           | 4.24  | 299.6                           | 10.04 | 374.5                           | 19.61 | 446.9                           | 33.34     | 498.6                            | 46.29     | 518.9                            | 52.18     |
| 4.5       | 0.265 | 168.5                           | 1.04  | 252.8                           | 3.51  | 337.0                           | 8.32  | 421.3                           | 16.24 | 502.8                           | 27.61     | 560.9                            | 38.34     | 583.8                            | 43.21     |
| 5         | 0.17  | 187.2                           | 0.67  | 280.9                           | 2.25  | 374.5                           | 5.33  | 468.1                           | 10.42 | 558.6                           | 17.71     | 623.3                            | 24.59     | 648.6                            | 27.72     |
| 5.6       | 0     | 209.7                           | 0     | 314.6                           | 0     | 419.4                           | 0     | 524.3                           | 0     | 625.7                           | 0         | 698.1                            | 0         | 726.5                            | 0         |

table 2 Calculated values of n and P as a function of  $\lambda$  and V for the VIRYA-1.02 rotor

The calculated values for n and P are plotted in figure 4. The optimum cubic line which is going through the tops of the  $P_{mech}$ -n curves is also given in figure 4.

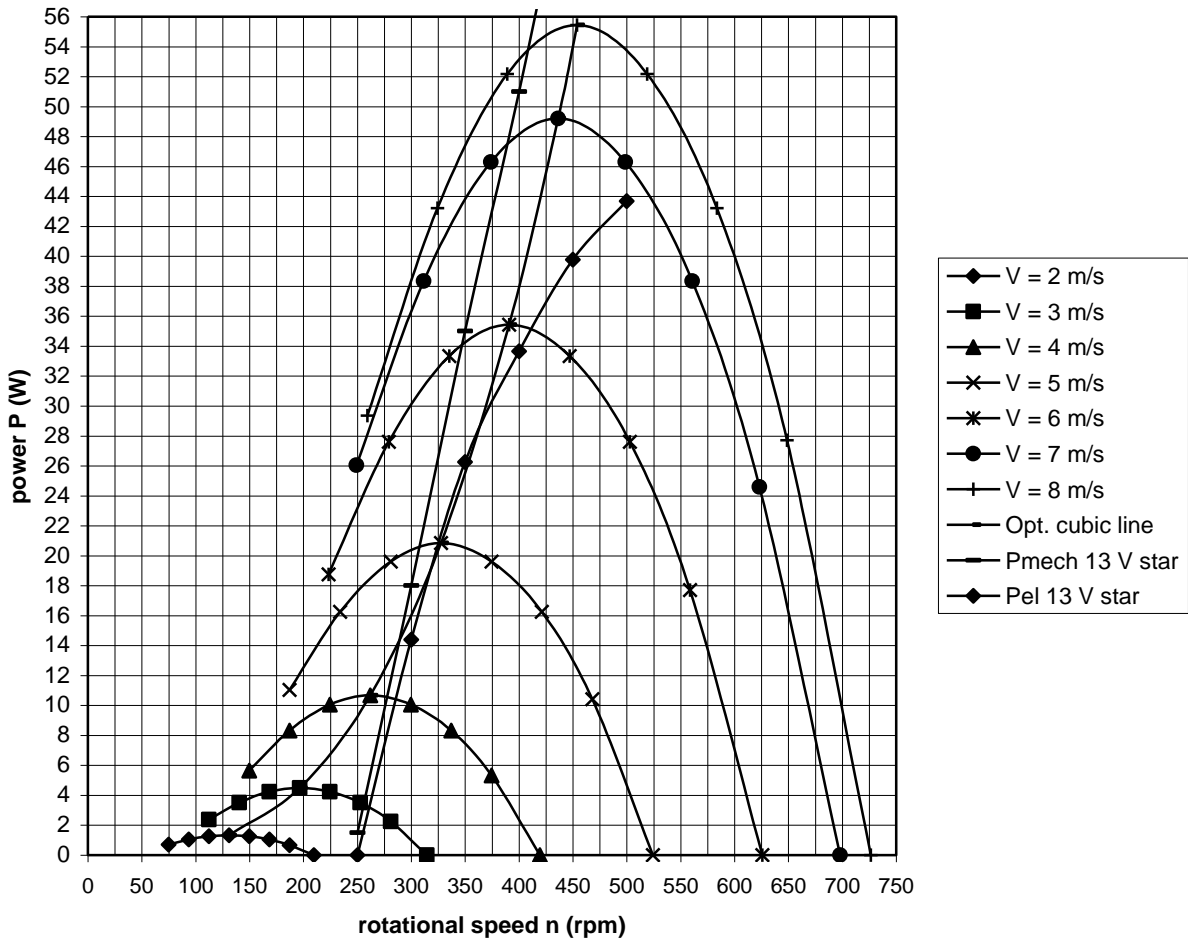


fig. 4 P-n curves and optimum cubic line of the VIRYA-1.02 rotor

A prototype of the generator has not yet been built (at June 2019), so measured characteristics of the generator for a 12 V battery load are not available. However, the  $P_{mech}$ -n and  $P_{el}$ -n curves for 13 V star are estimated and given in figure 5 of KD 626. These curves are copied in figure 4. The working point for a certain wind speed is the point of intersection of the  $P_{mech}$ -n curve of the generator and the P-n curve of the rotor for that wind speed. The  $P_{mech}$ -n curve intersects with the optimum cubic line at a wind speed of about 4.4 m/s. So the matching is perfect for this wind speed.

The matching is good for wind speeds in between 3 m/s and 8 m/s because the working point is lying a bit to the right side of the optimum cubic line for wind speeds in between 3 m/s and 4.4 m/s and a bit to the left side of the optimum cubic line for wind speeds above 4.4 m/s.

The corresponding electrical power  $P_{el}$  for a certain working point is found by going down vertically from the working point up to the point of intersection with the  $P_{el}$ - $n$  curve of the generator. This is done for all wind speeds and the values of  $P_{el}$  found this way are given in the  $P_{el}$ - $V$  curve of figure 5.

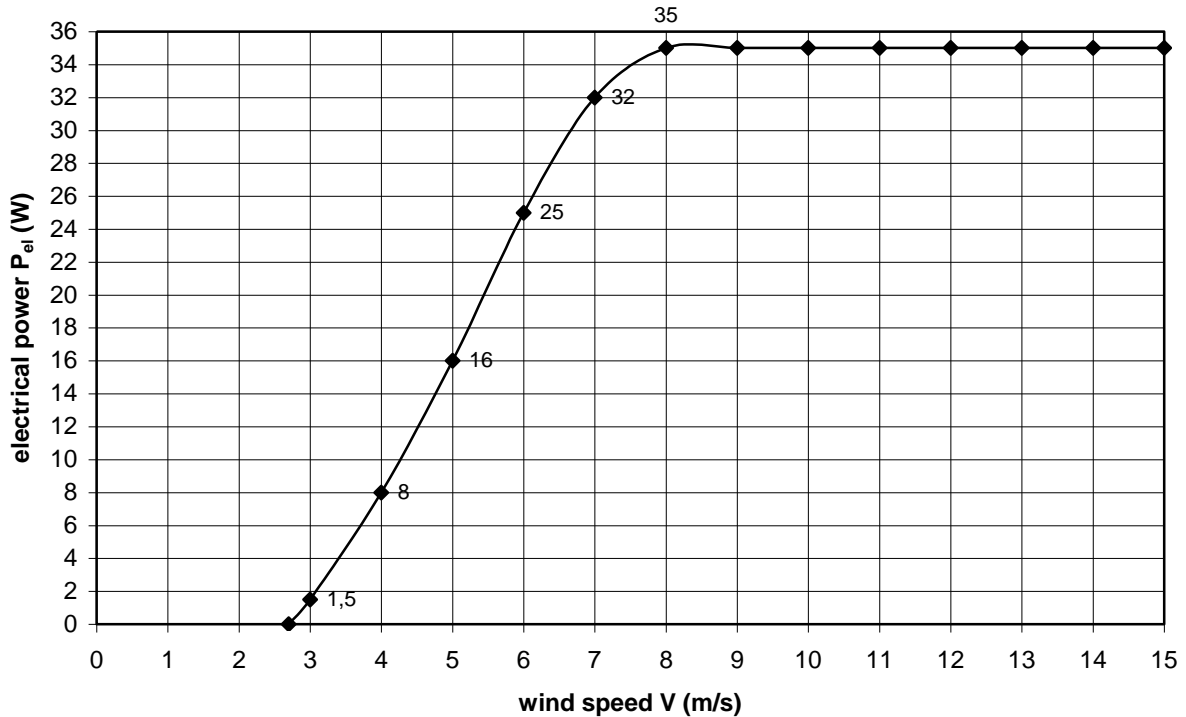


fig. 5 Estimated  $P_{el}$ - $V$  curve of the VIRYA-1.02 windmill for 12 V battery charging

The wind speed where the generation of power starts is called the cut in wind speed  $V_{cut\ in}$ . In the  $P_{el}$ - $V$  curve it can be seen that  $V_{cut\ in} = 2.7$  m/s. This is rather low. In chapter 4 it was calculated that the starting wind speed is 1.5 m/s. So there is no hysteresis in the  $P_{el}$ - $V$  curve.

The maximum electrical power is about 35 W which is acceptable for a rotor with a diameter of 1.02 m and a rated wind speed of 8 m/s. However, the  $P_{el}$ - $V$  curve is based on estimated  $P_{mech}$ - $n$  and  $P_{el}$ - $n$  curves. If a prototype of the generator is available, one should measure the generator for a 12 V battery load and check if the real curves are about the same as the estimated curves as used in June 2019. However, the generator has been measured in August 2019 and the measurements are given in chapter 6.

A maximum power of 35 W is that low that it is probably possible to use a large battery without a voltage controller and dump load which limits the maximum charging voltage if the battery is full.

The stainless steel hub plate ears are stronger than the aluminium blades of the VIRYA-1.04 rotor. Although the thickness of the blade is only 1 mm, it is stronger than a hub plate ear because the moment of resistance is increased a lot by the 15° bent sides. The strength of the VIRYA-1.04 rotor has been calculated in report KD 518 (ref. 7) and it was found that the VIRYA-1.04 rotor is strong enough. So the VIRYA-1.02 rotor will also be strong enough and separate calculations of the strength of the rotor will not be made.

## 6 Generator measurements

### 6.1 General

A prototype of the VIRYA-1.02 has been built by a teacher of a technical school in Rotterdam. This man wants to use this windmill for a project in Gambia for which the VIRYA-1.02 will be used to pump drinking water using a small 12 V electric pump. This use is described in report KD 672 (ref. 8) for the VIRYA-1 or the VIRYA-1.02 windmill.

Unfortunately the prototype of the VIRYA-1.02 generator wasn't made exactly according to the drawings which were valid at that time. It deviated at the following points:

- A The stator sheet was made out of 3 mm galvanised steel sheet but the outer geometry wasn't made dodecagonal as it is specified on drawing 1703-01 of the VIRYA-1.25AF. It was made hexagonal as it is now specified on drawing 1604-02 of the VIRYA-1 which can be found in report KD 679 (ref. 1). The reason why I made the steel stator sheet dodecagonal was that I was afraid than a hexagonal sheet would get 24 preference positions per revolution. However, it appeared that a hexagonal sheet gives no preference positions (if stainless steel screws are used to connect the coils). So now it is decided to make the sheet hexagonal in stead of dodecagonal. The VIRYA-1.25AF with a dodecagonal stator sheet is cancelled, also because it appeared that the matching in between rotor and generator isn't good enough.
- B The coil core is specified on drawing 1604-02 which can be found in report KD 679 (ref. 1). For the material it is specified polyacetal POM (Delrin, Ertacetal). However the coil cores were not made out of massive bar from this material but were made on a 3D printer and I don't know which material is used. For the original coil core, the front flange has a thickness of 1.3 mm and the back flange has a thickness of 0.7 mm. Both flanges have been made 1 mm for the prototype but this results in the same volume available for the coils. The coil winding has been made according to the specification so it is assumed that this modification has no influence of the generator characteristics.
- C In stead of a front wheel hub of a mountain bike, a back wheel hub was used. This hub has a threaded part for connection of the chain sprocket and the shaft is much longer. Therefore it wasn't possible to connect the generator to the available hub of the test rig. So for the measurements, I have used the original front wheel hub with the original armature sheet and the original magnets but for the stator I have used the hexagonal stator sheet with six coils and the chosen 3-phase rectifier.

The test rig is described in report KD 595 (ref. 9) for use in combination with an axial flux generator of Hefei Top Grand. This test rig is provided with a chain transmission with a reducing gear ratio. Therefore generators can be measured with a rather large maximum torque level. However, the expected maximum torque level of the VIRYA-1 and the VIRYA-1.02 generator is rather low and the generator can therefore be mounted directly to the shaft of the driving motor. This shaft was provided with an aluminium bush and the front flange of the generator housing was connected to this bush by six screws M4. The base sheet of the test rig is clamped in the vice of my work bench.

This test rig has been used earlier to measure the unloaded torque  $Q$  as a function of the rotational speed  $n$ . These measurements are described in chapter 8 of report KD 679 (ref. 1).

The VIRYA-1.02 will be used to charge a 12 V lead acid battery with a capacity of about 60 Ah. However such a battery wasn't available. Therefore I have used a battery charge controller with a voltage controller which is adjusted at a voltage of about 13 V. This is about the average charging voltage of a 12 V battery. So the measured characteristics will deviate only slightly from the characteristics for a real 12 V battery.

For the determination of the  $P_{\text{mech-n}}$ ,  $P_{\text{el-n}}$  and the  $\eta$ -n curves, one has to measure the torque  $Q$ , the rotational speed  $n$ , the DC voltage  $U$  and the DC current  $I$ . The rotational speed  $n$  has been measured with a laser rpm meter using a white dot on the hub of the driving motor. The voltage  $U$  and the current  $I$  have been measured with a digital universal meter.

As the generator hub is connected directly to the driving motor, the torque  $Q$  is the reaction torque needed to prevent that the stator sheet is rotating. The stator sheet is provided with a balanced lever with a length of the arm  $r = 0.141$  m. An accurate analogue balance is placed on the floor below the vice of the work bench. This balance has a maximum range of 5 kg for five rotations of the pointer. The scale of the balance has a line every 5 gram and the pointer can be read with an accuracy of about 2 gram. The balance is loaded with a mass of 4.565 kg. A thin rope is connected in between the lever and this mass such that the torque  $Q$  results in a pulling force in the rope. So the pointer turns backwards at increasing torque. The pulling force  $F$  is proportional to the decrease of the measured mass  $\Delta m$  as shown by the pointer of the balance. The torque  $Q$  is given by:

$$Q = F * r \quad (\text{Nm}) \quad (10)$$

In this formula,  $F$  is the force in the rope in N and  $r$  is the radius of the lever in m. However, a balance isn't measuring the force  $F$  in N but the mass  $m$  in kg. The relation in between  $F$ ,  $\Delta m$  and the acceleration of gravity  $g$  ( $g = 9.81 \text{ m/s}^2$ ) is given by:

$$F = \Delta m * g \quad (\text{N}) \quad (11)$$

(10) + (11) gives:

$$Q = \Delta m * g * r \quad (\text{Nm}) \quad (12)$$

The mechanical power  $P_{\text{mech}}$  is given by:

$$P_{\text{mech}} = Q * \Omega \quad (\text{W}) \quad (13)$$

In this formula,  $Q$  is the torque in Nm and  $\Omega$  is the angular velocity in rad/s. The relation in between the angular velocity  $\Omega$  (rad/s) and the rotational speed  $n$  (rpm) is given by:

$$\Omega = \pi * n / 30 \quad (\text{rad/s}) \quad (14)$$

(12) + (13) + (14) gives:

$$P_{\text{mech}} = \Delta m * g * r * \pi * n / 30 \quad (\text{W}) \quad (15)$$

Substitution of  $g = 9.81 \text{ m/s}^2$ ,  $r = 0.141$  m and  $\pi = 3.14159$  in formula 15 gives:

$$P_{\text{mech}} = 0.1448 * \Delta m * n \quad (\text{W}) \quad (16)$$

The supplied electrical power  $P_{\text{el}}$  is given by:

$$P_{\text{el}} = U * I \quad (\text{W}) \quad (17)$$

In this formula  $U$  is the DC voltage and  $I$  is the DC current. So the losses in the rectifier are incorporated in the generator efficiency. The generator efficiency  $\eta$  in % is given by:

$$\eta = 100 * P_{\text{el}} / P_{\text{mech}} \quad (\%) \quad (18)$$

## 6.2 Measuring results

First the unloaded DC voltage  $U$  was measured for rectification in star as a function of the rotational speed. The measured  $U$ - $n$  curve is given in figure 6.

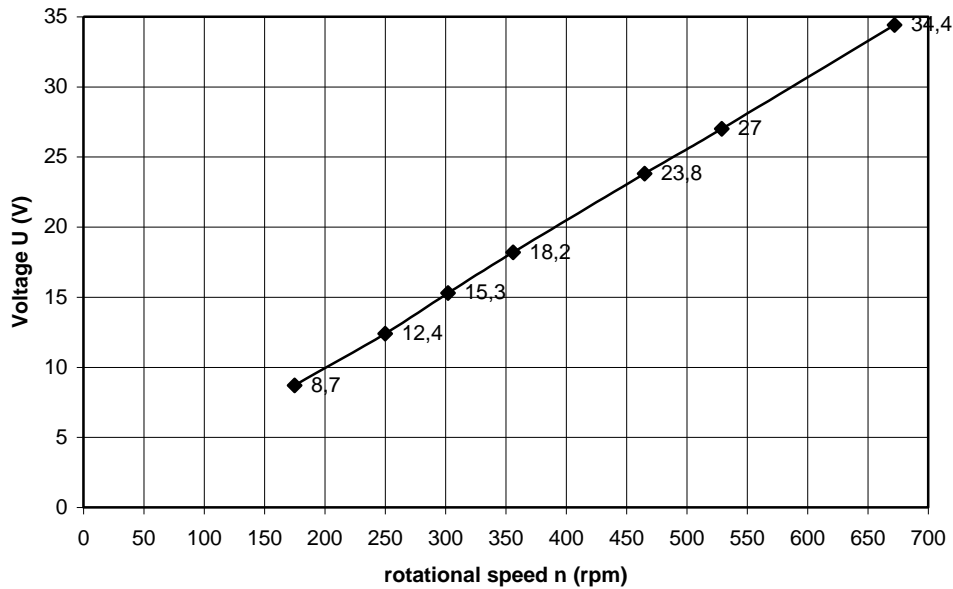


fig. 6 Open voltage  $U$  as a function of the rotational speed  $n$  for star rectification

In figure 6 it can be seen that the  $U$ - $n$  curve is a straight line and that the open voltage  $U$  is 12.4 V at  $n = 250$  rpm. The extended line is intersecting with the  $x$ -axis at about  $n = 10$  rpm. In an earlier design report of the VIRYA-1 rotor it was determined that the winding of one coil should have 230 turns per coil for a wire thickness of 0.56 mm. It was expected that a complete winding with six coils would have an open voltage of 12.5 V at a rotational speed of 250 rpm if the winding is rectified in star. The measured open voltage is 12.4 V for  $n = 250$  rpm, so the chosen number of turns per coil is correct.

Next the generator was measured, connected to a battery charge controller adjusted at a voltage of about 13 V. The measuring points and the calculated values for  $Q$ ,  $P_{\text{mech}}$ ,  $P_{\text{el}}$  and  $\eta$  are given in table 3. The  $\eta$ - $n$  curve is given in figure 7.

| n (rpm) | m <sub>pointer</sub> (kg) | Δm (kg) | Q (Nm) | P <sub>mech</sub> (W) | U <sub>DC</sub> (V) | I <sub>DC</sub> (A) | P <sub>el</sub> (W) | η (%) |
|---------|---------------------------|---------|--------|-----------------------|---------------------|---------------------|---------------------|-------|
| 157     | 4.545                     | 0.020   | 0.028  | 0.45                  | 6.8                 | 0                   | 0                   | -     |
| 250     | 4.535                     | 0.030   | 0.041  | 1.09                  | 12.2                | 0                   | 0                   | -     |
| 273     | 4.525                     | 0.040   | 0.055  | 1.58                  | 13.05               | 0.02                | 0.26                | 16.5  |
| 290     | 4.495                     | 0.070   | 0.097  | 2.94                  | 13.13               | 0.10                | 1.31                | 44.6  |
| 305     | 4.455                     | 0.110   | 0.152  | 4.94                  | 13.14               | 0.19                | 2.50                | 51.5  |
| 320     | 4.427                     | 0.138   | 0.191  | 6.39                  | 13.15               | 0.27                | 3.55                | 55.6  |
| 359     | 4.333                     | 0.232   | 0.321  | 12.06                 | 13.15               | 0.53                | 6.97                | 57.8  |
| 390     | 4.261                     | 0.304   | 0.420  | 17.17                 | 13.16               | 0.73                | 9.61                | 56.0  |
| 431     | 4.166                     | 0.399   | 0.552  | 24.90                 | 13.16               | 0.98                | 12.90               | 51.8  |
| 479     | 4.053                     | 0.512   | 0.708  | 35.51                 | 13.17               | 1.32                | 17.38               | 48.9  |
| 515     | 3.970                     | 0.595   | 0.823  | 44.37                 | 13.18               | 1.58                | 20.82               | 46.9  |
| 564     | 3.870                     | 0.695   | 0.961  | 56.76                 | 13.18               | 1.86                | 25.51               | 44.9  |
| 601     | 3.790                     | 0.775   | 1.072  | 67.44                 | 13.18               | 2.20                | 29.00               | 43.0  |

Table 3 Measured and calculated values of the VIRYA-1.02 generator

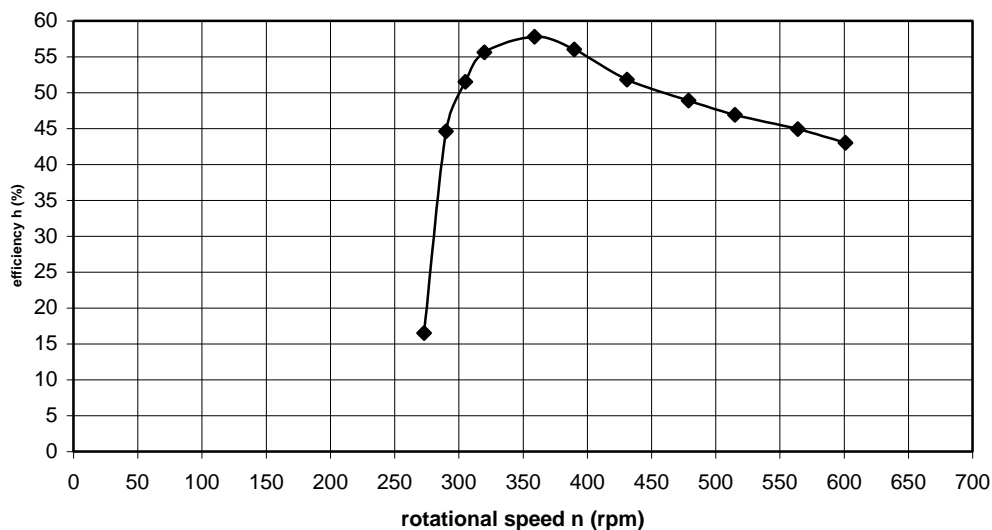


fig. 7 Measured  $\eta$ - $n$  curve of the VIRYA-1.02 generator for 12 V battery charging.

Next figure 4 is copied as figure 8 but the estimated  $P_{\text{mech}}-n$  and  $P_{\text{el}}-n$  curves are replaced by the measured  $P_{\text{mech}}-n$  and  $P_{\text{el}}-n$  curves for 13 V star. A new  $P_{\text{el}}-V$  curve is derived using the measured  $P_{\text{mech}}-n$  and  $P_{\text{el}}-n$  curves and this new  $P_{\text{el}}-V$  curve is given in figure 9. For a real 12 V battery, the maximum charging voltage will be higher than 13 V at high powers resulting in a somewhat higher efficiency and a somewhat higher maximum power. The  $P_{\text{el}}-V$  curve is corrected for this effect at high wind speeds.

If the estimated and the measured  $P_{\text{mech}}-n$  and  $P_{\text{el}}-n$  curves are compared, it can be seen that the measured curves are lying a lot lower than the estimated curves. The rotor isn't running at the design tip speed ratio of 3.5 but at a tip speed ratio somewhat higher than 4 because the torque is lower than expected. But the matching is still acceptable.

The  $P_{\text{mech}}-n$  curve will shift to the left if a winding with more turns per coil is used. However, this will result in a longer and thinner wire and the copper losses will therefore increase and this results in decrease of the generator efficiency. I therefore think that the chosen and tested winding is still rather optimal for the VIRYA-1.02. The matching will be better for the 2-bladed VIRYA-1 rotor as this rotor has a design tip speed ratio of 4.25.

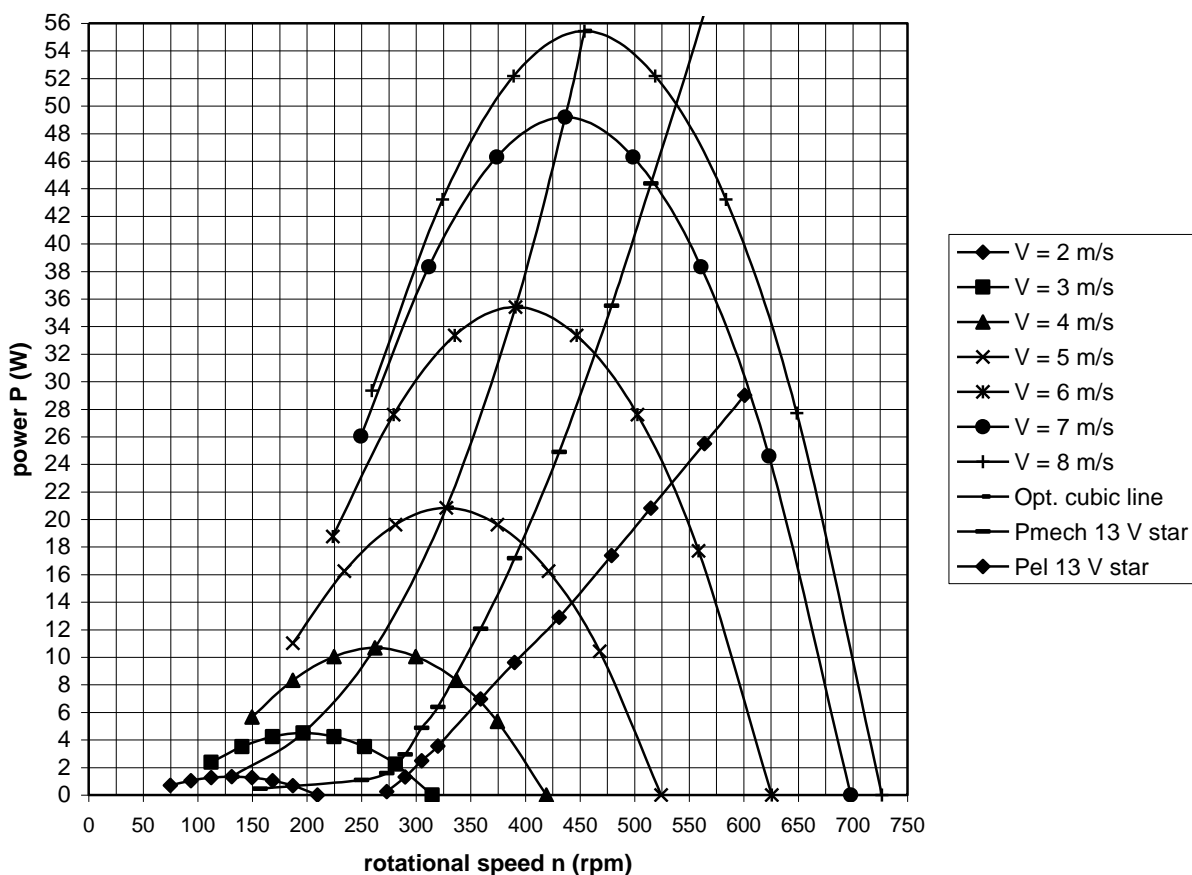


fig. 8 Estimated  $P$ - $n$  curves and optimum cubic line of the VIRYA-1.02 rotor, measured  $P_{\text{mech}}-n$  and  $P_{\text{el}}-n$  curves.

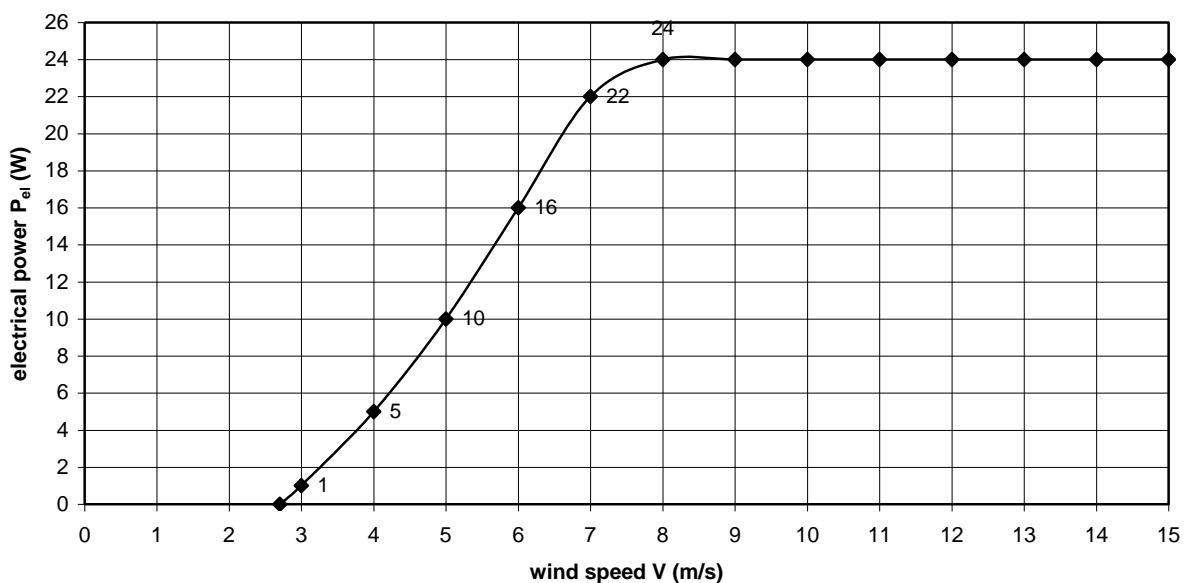


fig. 9  $P_{\text{el}}-V$  curve of the VIRYA-1.02 for measured generator characteristics

The  $P_{\text{el}}-V$  curve is also lying lower than the estimated curve as given in figure 5 but for wind speeds above about 3.6 m/s, it is much better than the  $P_{\text{el}}-V$  curve of the VIRYA-1.04 with a Nexus hub dynamo (see figure 5 report KD 518, ref. 7).

## 7 Discussion of the measuring results

The  $\eta$ - $n$  curve as given in figure 7 is a bit disappointing as the maximum efficiency is only about 0.58 at a rotational speed of about 350 rpm. In figure 8 it can be seen that this rotational speed is reached at a wind speed of about 4.3 m/s for the VIRYA-1.02.

If the generator is used for the 2-bladed VIRYA-1, it can be seen in figure 5 of report KD 679 (ref. 1) that a rotational speed of 350 rpm is reached at about a wind speed of 5 m/s. So for both windmills the maximum efficiency is reached at a wind speed which will happen very often.

In figure 8 it can be seen that the maximum rotational is reached for the point of intersection of the  $P_{\text{mech}}$ - $n$  curve of the generator with the  $P$ - $n$  curve of the rotor for  $V = 8$  m/s. This point is lying at about a rotational speed of 540 rpm and the mechanical power is about 50 W for the VIRYA-1.02. The maximum electrical power is about 23 W so the efficiency is  $23 / 50 = 0.46$  for the maximum rotational speed of the VIRYA-1.02. In table 3 it can be seen that the voltage at this rotational speed is 13.18 V. For a real battery, the maximum charging voltage may be a little higher than 13.18 V resulting in a higher generator efficiency. In the  $P_{\text{el}}$ - $V$  curve of figure 9 it is therefore assumed that the maximum electrical power is 24 W.

If the generator is used for the 2-bladed VIRYA-1, it can be seen in figure 5 of report KD 679 (ref. 1) that the maximum rotational speed is about 575 rpm for  $V = 8$  m/s and that the mechanical power is about 60 W. The maximum electrical power is about 27 W, so the efficiency is  $27 / 60 = 0.45$  for the maximum rotational speed of the VIRYA-1. The real voltage during the measurements can be read from table 3 and it can be seen that  $U_{\text{DC}} = 13.18$  V at  $n = 575$  rpm. For a real battery, the maximum charging voltage may be a little higher than 13.18 V but 27 W is maintained as the maximum power of the VIRYA-1 (see  $P_{\text{el}}$ - $V$  curve, figure 6 of KD 679).

So the highest electrical power is generated for the VIRYA-1 and the measuring results are therefore discussed for the generator if it is used for the VIRYA-1 for a rotational speed of 575 rpm. The mechanical power at  $n = 575$  rpm is about 60 W and the electrical power is about 27 W, so 33 W is lost. So where this power is lost? There are five possible places being:

- 1) Bearing friction
- 2) Aerodynamic friction of the armature
- 3) Heat losses in the 3-phase rectifier
- 4) Iron losses in the steel stator sheet
- 5) Copper losses in the stator winding

The front wheel hub of a mountain bike has no seal at the bearings and the ball bearings are running very light so I think that the bearing friction can be neglected. The aerodynamic friction of the armature spinning round in air is also very low at a rotational speed of 575 rpm so I think that the aerodynamic friction can be neglected too. So what remains are the losses given at point 3, 4 and 5.

If the generator supplies an electrical power of 27 W at a voltage of 13.18 V it can be calculated that the current  $I = 27 / 13.18 = 2.05$  A. The voltage drop over a 3-phase rectifier with silicon diodes is about 1.4 V. So the heat losses in the rectifier are about  $2.05 * 1.4 = 2.9$  W.

The open voltage is given in figure 6 but the unloaded torque  $Q$  has not been measured at that measuring date. However, the unloaded torque has been measured earlier for a 3 mm steel stator sheet. The unloaded  $Q$ - $n$  curve is given in figure 7 of KD 679 (ref. 1). In this figure it can be seen that  $Q = 0.105$  N for  $n = 575$  rpm. As  $P = Q * n * \pi / 30$ , it can be calculated that  $P = 6.3$  W for  $n = 575$  rpm.

So the sum of the losses in the rectifier and the iron losses in the stator sheet is  $2.9 + 6.3 = 9.2$  W. This means that about  $33 - 9.2 = 23.8$  W is dissipated in the copper of the stator winding due to  $I^2 * R$  losses. It will now be checked if this is about correct.

The generator has a 3-phase winding which is rectified in star. Star rectification of a 3-phase winding is explained in chapter 3.2.1 of report KD 340 (ref. 10). In figure 7 of KD 340 it can be seen that the current is flowing only through two of the three phases. Every phase has two coils and so the current is flowing only through four of the six coils.

A coil is specified on drawing 1604-02 which is given in the end of report KD 679 (ref. 1). A coil has a polyacetal core with two flanges. The inside diameter of the copper winding is 27 mm. The outside diameter of the copper winding is about the same as the outer flange diameter and so 45 mm. So the average diameter of the copper winding is about  $(27 + 45) / 2 = 36$  mm. So the average circumference of one turn is about  $\pi * 36 = 113$  mm.

A coil has a winding with 230 turns per coil so the total wire length of one coil is  $230 * 113 = 25990$  mm, so about 26 m. So the total wire length  $l$  of four coils connected in series is  $4 * 26 = 104$  m.

The wire has a thickness of 0.56 mm so the cross sectional area  $A$  of the wire is  $\pi/4 * 0.56^2 = 0.246$  mm<sup>2</sup>. A copper wire has a resistance  $R$  which is given by:

$$R = \rho * l / A \quad (\Omega) \quad (19)$$

$\rho$  is the specific resistance of copper which is about 0.0175  $\Omega \cdot \text{mm}^2/\text{m}$  for a temperature of 20° C. The specific resistance increases by the temperature but this effect is neglected as the temperature rise of the coil will be limited at a heat dissipation of about 24 W.  $l$  is the length of the wire in m.  $A$  is the cross sectional area of the wire in mm<sup>2</sup>.

Substitution of  $\rho = 0.0175$   $\Omega \cdot \text{mm}^2/\text{m}$ ,  $l = 104$  m and  $A = 0.246$  mm<sup>2</sup> in formula 19 gives that  $R = 7.4$   $\Omega$ . The maximum current was calculated earlier and it was found that  $I = 2.05$  A. So the  $I^2 * R$  losses in the winding are  $2.05^2 * 7.4 = 31.1$  W. This is even 7.3 W higher than the 23.8 W which was found if the total loss of 33 W is reduced by the losses in the 3-phase rectifier and in the iron of the stator. How can this be possible?

It might be that the losses in the stator sheet are smaller when a current is flowing because this current results in decrease of the magnetic flux flowing through the coils and through the iron. It might also be that the voltage drop over the rectifier is a bit smaller than 1.4 V resulting in smaller rectifier losses.

It might be that outer diameter of a coil is somewhat smaller than 45 mm resulting in a real length of the copper wire of one coil which is shorter than 26 m. It might also be that the cross sectional area of the wire is a little larger than 0.246 mm<sup>2</sup>. These two differences would result in a lower resistance of the winding and therefore in lower copper losses. But these calculations show clearly that most of the power is lost in the winding and that it is correct to neglect the bearing losses and the aerodynamic losses.

This simple 8-pole PM-generator has a rather long air gap in between the north and the south poles of the armature. This long air gap results in strong decrease of the magnetic flux flowing through the coils but this decrease is less than if a synthetic stator sheet would be used. The rather low magnetic flux through the coils makes that coils with a large number of turns per coil are needed to get a sufficient high voltage for 12 V battery charging and within a limited space, only a small wire diameter can be used. But although this generator has a rather low efficiency for the rpm range for which it is used in the wind turbine, the maximum power output is still much higher than for the VIRYA-1.04 with a Nexus hub dynamo. Therefore I think that this generator is still a reasonable option for a very small wind turbine like the VIRYA-1.02 or the VIRYA-1.

## 8 Ideas about an alternative stator for the VIRYA-1.02

The 8-pole generator of the 2-bladed VIRYA-1 windmill is described in report KD 679 (ref. 1). The generator drawings are given on drawing 1604-01 and 1604-02 which are given in appendix 1 of KD 679. The VIRYA-1 generator is also used for the 3-bladed VIRYA-1.02.

The matching of this generator with the VIRYA-1 rotor is shown in figure 5 of KD 579. In this figure it can be seen that the matching is very good because the  $P_{\text{mech-n}}$  curve of the generator is lying close to the optimum cubic line of the rotor. The matching of this generator with the VIRYA-1.02 generator is shown in figure 8 of this reports KD 578. In this figure it can be seen that the matching isn't optimal because there is a rather large distance in between the  $P_{\text{mech-n}}$  curve and the optimum cubic line of the rotor. The main reason why the matching of the VIRYA-1.02 is worse than for the VIRYA-1, is that the VIRYA-1.02 has a design tip speed ratio of 3.5 and that the VIRYA-1 has a design tip speed ratio of 4.25.

The  $P_{\text{el-V}}$  curve of the VIRYA-1 is given in figure 6 of KD 579. The  $P_{\text{el-V}}$  curve of the VIRYA-1.02 is given in figure 9 of KD 578. If both curves are compared it can be seen that the maximum power of the VIRYA-1 is 27 W and that it is 24 W for the VIRYA-1.02. So although the VIRYA-1.02 has a slightly larger rotor diameter it has a lower maximum power. This is caused by the fact that the matching is worse for the VIRYA-1.02 but also because the VIRYA-1.02 has a lower maximum  $C_p$  than the VIRYA-1. This is because the VIRYA-1.02 uses blades with  $15^\circ$  folded sides but the VIRYA-1 uses a better 7.14 % cambered airfoil.

The matching of the generator with the VIRYA-1.02 rotor can be improved if the  $P_{\text{mech-n}}$  curve of the generator could move to the left. This can be realised by choosing a winding with more turns per coil and a smaller wire diameter because the open battery voltage will then be reached at a lower rotational speed. However, increase of the number of turns per coil will result in a higher resistance of the wire and this will result in a lower generator efficiency. This will especially reduce the power at high currents so the maximum power will be lower.

Another option is to make the magnetic field stronger which is flowing through the coils. The magnetic flux depends strongly on the air gap  $t_2$  in between the magnets and the steel stator sheet. The flux density in the air gap is calculated in chapter 3 of KD 679 and it was found that  $B_{r \text{ eff}} = 0.595 \text{ T}$  for  $t_2 = 13 \text{ mm}$ . The coil geometry is given on drawing 1604-02. The coil core has a 1.3 mm flange at the front side and a 0.7 mm flange at the back side. The flange at the back side can be thinner because bending outwards of this flange is prevented by the steel stator sheet. A way to make the coils thinner is to cancel both flanges. However, to prevent that the coil falls apart when it is removed from the winding thorn, a thin layer of epoxy has to be put on each layer of the coil during the winding process. The coil should be removed from the winding thorn only after hardening of the epoxy. The steel stator sheet has to be covered with a thin about 0.05 mm thick plastic layer to prevent possible short-circuit in between wires of the coil and the sheet. But the thickness of the air gap with this thinner 10 mm wide coil can be reduced from  $t_2 = 13 \text{ mm}$  up to  $t_2 = 11 \text{ mm}$ . If the flux density in the air gap is calculated again using formula 1 of KD 579, it is found that  $B_{r \text{ eff}} = 0.647$ . So  $B_{r \text{ eff}}$  increases by a factor  $0.647 / 0.595 = 1.087$ . It might be that the real factor is even larger than the calculated factor because a smaller air gap will also make that relatively less magnetic flux lines are flowing from a north to a south pole without passing the steel stator sheet.

Another way to increase the magnetic flux is to use bigger magnets size  $\phi 29 * 10 \text{ mm}$ . These magnets are supplied by the same Polish supplier as the original magnets and the magnets costs for eight magnets are only € 2 higher. The distance in between the armature sheet and the stator sheet must now be 21 mm for 10 mm wide coils. So increasing the magnet area and reducing the air gap will result in increase of the magnetic flux and therefore in increase of the open voltage at a certain rotational speed. This means that the  $P_{\text{mech-n}}$  curve will shift to the left resulting in a better matching for the VIRYA-1.02. The winding is unchanged so the copper losses for a certain current won't increase. The stronger magnetic field will give a certain increase of the unloaded Q-n curve as given in figure 7 of KD 679 but this is no problem for the VIRYA-1.02 rotor as the starting torque coefficient is high enough.

## 9 References

- 1 Kragten A. Development of an 8-pole, 3-phase axial flux permanent magnet generator for the VIRYA-1 windmill using a bicycle hub and 8 neodymium magnets size  $\phi 25 * 12$  mm and a stator sheet made out of galvanised steel sheet, August 2019, reviewed December 2019, free public report KD 679, engineering office Kragten Design, Populierenlaan 51, 5492 SG Sint-Oedenrode, The Netherlands.
- 2 Kragten A. Calculations executed for the 3-bladed rotor of the VIRYA-1.04 windmill ( $\lambda_d = 3.5$ , 7.14 % cambered, aluminium blades) meant to be coupled to a Nexus hub dynamo (with free manual), January 2013, reviewed May 2013, free public report KD 518, engineering office Kragten Design, Populierenlaan 51, 5492 SG Sint-Oedenrode, The Netherlands.
- 3 Kragten A. Manual of electricity generating windmill VIRYA-1.04, February 2013, reviewed May 2013, free public manual, engineering office Kragten Design, Populierenlaan 51, 5492 SG Sint-Oedenrode, The Netherlands.
- 4 Kragten A. Rotor design and matching for horizontal axis wind turbines, July 1999, free public rapport KD 35, engineering office Kragten Design, Populierenlaan 51, 5492 SG Sint-Oedenrode, The Netherlands.
- 5 Kragten A. The 7.14 %, 10 % and 12.5 % cambered plate as airfoil for windmill rotor blades, Aerodynamic characteristics, geometry, moment of inertia I and moment of resistance W, November 2008, free public report KD 398, engineering office Kragten Design, Populierenlaan 51, 5492 SG Sint-Oedenrode, The Netherlands.
- 6 Kragten A. Determination of  $C_q$  for low values of  $\lambda$ . Deriving the  $C_p-\lambda$  and  $C_q-\lambda$  curves of the VIRYA-1.02.8D rotor, July 2002, free public report KD 97, engineering office Kragten Design, Populierenlaan 51, 5492 SG Sint-Oedenrode, The Netherlands.
- 7 Kragten A. Calculations executed for the 3-bladed rotor of the VIRYA-1.04 windmill ( $\lambda_d = 3.5$ , 7.14 % cambered aluminium blades) meant to be coupled to a Nexus hub dynamo. January 2013, reviewed May 2013, free public report KD 518, engineering office Kragten Design, Populierenlaan 51, 5492 SG Sint-Oedenrode, The Netherlands.
- 8 Kragten A. Use of the VIRYA-1, the VIRYA-1.02 or the VIRYA-1.04 for pumping of drinking water using a 12 V battery and a pump with a 12 V DC motor. May 2019, reviewed August 2019, free public report KD 672, engineering office Kragten Design, Populierenlaan 51, 5492 SG Sint-Oedenrode, The Netherlands.
- 9 Kragten A. Measurements performed on a Chinese axial flux generator of Hefei Top Grand model TGET165-0.15 kW-500R for a 12 V battery load. September 2015, free public report KD 595, engineering office Kragten Design, Populierenlaan 51, 5492 SG Sint-Oedenrode, The Netherlands.
- 10 Kragten A. Rectification of 3-phase VIRYA windmill generators. May 2007, reviewed April 2017, free public report KD 340, engineering office Kragten Design, Populierenlaan 51, 5492 SG Sint-Oedenrode, The Netherlands.

Appendix 1 Drawing VIRYA-1.02 rotor,  $\lambda_d = 3.5$ ,  $B = 3$

